Electronic Supplementary Information (ESI)

Probing the Properties of Size Dependence and Correlation for Tantalum Clusters: Geometry, Stability, Vibrational Spectra, Magnetism and Electronic Structure

Xibo Li[1,*], Yuqi Chen[2], Pradip Basnet[3], Jiangshan Luo[1] and Hongyan Wang[2,*]

1. Science and Technology on Plasma Physics Laboratory, Laser Fusion Research Center, China Academy of Engineering Physics, P. O. Box 919-987, Mianyang, Sichuan 621999, China

2. School of Physical Science and Technology, Southwest Jiaotong University, Chengdu, Sichuan 610031, China

3. School of Materials Science and Engineering, Georgia Institute of Technology, Atlanta, GA 30318, USA

* Corresponding authors, E-mail: xiboli@foxmail.com (Xibo Li), hongyanw@swjtu.edu.cn (Hongyan Wang)

1 Computational Details

1.1 DFT Method

The all-electron relativistic results for the TMs clusters are generally in agreement with the results given by relativistic effective core potential (RECP).[1] In LANL2DZ basis set, the core electrons are frozen by RECP (scalar relativistic effect is considered) and the valence electrons are treated by a double-zeta basis set.[2] On the other hand, the spin–orbit (SO) effect was averaged out or only effective SO was considered. Since SO effect could be very important for heavy metals like Ta, the results may differ compared with the case that SO effect was considered explicitly. The valence electrons of Ta are considered to be $5s^2 5p^6 5d^3 6s^2$ in LANL2DZ basis set. It is well known that the geometries and electronic properties are quite sensitive to the exchange and correlation functional used in the DFT method for TM clusters. We have dealt with different TM clusters by using different functional, such as, generalized gradient approximation (GGA) with the PW91 functional for gold cluster[3] and BP86 functional for yttrium clusters.[4] There are different opinions for which functional is appropriate to deal with the dimer and trimer of tantalum in previous studies. A systemic DFT study on several 5*d*-electron element dimers

has been reported by Sun *et al.*[1] Their results show that the BP86 and PBEPBE functionals are generally successful in describing the 5*d*-electron dimers, and the hybrid functionals are not fit to describe Ta_2 dimer. However, Wang *et al.*,[5] Heaven *et al.*,[6] and Wu *et al*[7] concluded that the hybrid functionals of B3LYP or B3P86 gave superior results in terms of spectroscopic constant properties when directly compared to experimental results for dimer or trimer of tantalum.

Therefore, to test the reliability of our calculation, the spectroscopic constant properties of the Ta_2 and Ta_3 cluster are calculated at the B3LYP/LANL2DZ level and compared with the previous experimental and theoretical data. The spin quintet state ($^5\sum_u$) is the ground state for Ta_2 dimer agrees with previous DFT studies,[1,7] but is different from its congeners V_2 and Nb_2. The triplet state and singlet state were predicted to be the ground state for V_2[8]and Nb_2[9], respectively. The computed dissociation energy of 2.896 eV for Ta_2 is slightly lower than the measured value of 4±1 eV.[10] The computed ionization potentials of Ta_2 with 6.144 eV is well reproduced in comparison with the measured value of 5.98-6.42 eV.[11] The obtained vibrational frequencies of 285.4 cm^{-1} is only 14.8cm^{-1} lower than the resonance Raman spectroscopy measured value 300.2 cm^{-1}.[12] Until now, no experimental data have been available for the equilibrium bond length of Ta_2. However, our calculated value (2.260 Å) compares favorably with the result obtained by using *Guggenheimer's* rule, which is 2.23 Å.[13]

At the B3LYP/LANL2DZ level, our results show that the ground state for Ta_3 trimer is an equilateral triangle with three bond lengths 2.508Å at a spin sextet state ($^6A'$). Two competitive candidates for the ground state of Ta_3 are found, the quartet state and doublet state with isosceles triangle (C_{2v} symmetry) are 0.094 eV and 0.129 eV higher in energy than the sextet state, respectively. The linear structures of Ta_3 cluster is unstable which is separated by a large energy gap of 2.679 eV from the lowest-energy structure. The current structures and energetics for Ta_3 agree in general with those from a previous DFT study at the GGA level by using DMOL^3 package.[14] A symmetric Ta-Ta stretching frequency (257.23 cm^{-1}) is obtained at our used DFT method, agrees with the resonant Raman spectrum experiment value (251.7 cm^{-1}).[15] The calculated ionization potential of Ta_3 trimer is 5.829 eV, also agrees with the reported two

independent experimental results (5.60 eV[16] and 5.58±0.05 eV[11], respectively). The obtained electron affinity of 1.003 eV is only a little lower than the photoelectron spectroscopy (PES) measured value of 1.35±0.03 eV.[5]

When the cluster has less than six atoms, the default self-consistent field convergence of 10^{-8} is used. For the larger clusters ($n \geq 6$), the computation cannot converge except to a 10^{-6} tolerance. The thresholds for convergence are 0.000 45 and 0.0003 a.u. for the maximum force and root-mean-square force, respectively. The calculated total energies of isomers are all corrected with zero-point vibrational energy. The set of starting configurations chosen is extensive enough to ensure sufficiently thorough exploration of the cluster potential energy surfaces. To search the lowest energy structures of tantalum clusters, lots of initial isomers, which include one-, two- and three-dimensional (3D) configurations, had been taken into account in our geometry optimizations. The structures considered for initial optimizations are constructed by using two different routes. In the first one, we employ the reported results of other transition metal clusters as the initial structures, including all isomers found in reasonable geometries of neutral and charged Vanadium, Niobium, Tantalum clusters in other previous works. In the second route, the initial geometries of a certain size Ta_n are generated from the lowest lying isomers of a cluster of size n-1 or n+1 by adding or subtracting an extra Ta atom systematically at all possible positions. We also add or subtract two atoms from a cluster of size n to obtain geometry for a cluster of size n+2 or n-2. This procedure can also be called a successive growth algorithm.[17] Then, all possible isomeric structures obtained from above step is reoptimized by setting various spin multiplicities to determine their spin ground state.

To confirm the stability of structures the vibrational frequencies are analyzed. If an imaginary vibrational mode is found, a relaxation of the structure is performed until the true local minimum is actually obtained. All the geometrical structures obtained in this work are stable. Harmonic vibrational frequencies are computed also used to simulate vibrational spectra of clusters in this paper. Vibrational frequencies are computed by determining the second derivatives of the energy with respect to the Cartesian nuclear coordinates and then transforming to mass-weighted coordinates. The vibrational

spectrum directly come from GaussView 5.08 software which combined with Gaussian 03 without broadening and scaling. Please note that the intensity values are relative to the highest value in the present set, and bear no precise relationship to experimental band intensities. We use Multiwfn program (http://sobereva.com/multiwfn/), which is the open-source and an extremely powerful electronic wavefunction analysis to calculate the deformation charge density and the projected DOS. The wavefunction information obtained from the Gaussian formatted check file ***.fch.

1.2 Definition of Reactivity Descriptors

We computed the vertical ionization potentials (*VIP*) using the formula:

$$VIP = \mathrm{E(Ta}_n)^+ - \mathrm{E(Ta}_n)$$

where $\mathrm{E(Ta}_n)^+$ and $\mathrm{E(Ta}_n)$ are the ground state energy of the cationic clusters at the optimized geometry of the cation and the optimized geometry of neutral cluster, respectively.

The adiabatic and vertical electron affinities (*VEA*) are calculated from the equation:

$$VEA = \mathrm{E(Ta}_n) - \mathrm{E(Ta}_n)^-$$

where $\mathrm{E(Ta}_n)$ and $\mathrm{E(Ta}_n)^-$ is the ground state energy of the optimized geometry of neutral cluster and the anionic clusters at the optimized geometry of anion, respectively.

In DFT, the molecular chemical hardness (η) for the *N*-electron system with total energy *E* and external potential $v(r)$ are defined as the following second derivatives of the energy with respect to *N*: [18,19]

$$\eta = \frac{1}{2}\left(\frac{\partial^2 E}{\partial N^2}\right)_{v(r)} = \frac{1}{2}\left(\frac{\partial \mu}{\partial N}\right)_{v(r)}$$

It has been customary to employ a finite difference approximation to the derivatives, using the energies of *N*, (*N*+1), and (*N*-1) electron systems and the Koopmans theorem;[18] thus, η is calculated through the following approximate equation:

$$\eta \approx (VIP - VEA)/2$$

where *VIP* and *VEA* are the first vertical ionization energy and electron affinity of the chemical species, respectively.

1.3 Finite Field Treatment

The static response properties of a molecule can be defined in two different ways. The field-dependent energy $E(F)$ can be expanded in a series

$$E(F) = E(0) - \sum_i \mu_i F_i - \frac{1}{2}\sum_{ij} \alpha_{ij} F_i F_j - \cdots\cdots$$

where $E(0)$ is the total energy of the molecular system in the absence of the electric field, the quantities F_i are components of the applied field in different directions ($i, j = x; y; z$), and μ_i and α_{ij} are components of the static dipole moment and polarizability tensor, respectively.

Alternatively, the static response properties of a molecule can be defined by expanding the field-dependent dipole moment, calculated from the field-induced charge distribution, as a series of the external electric field

$$\mu_i(F) = -\frac{\partial E(F)}{\partial F_i} = \mu_i(0) + \sum_j \alpha_{ij} F_j + \cdots\cdots$$

The equivalence of these two definitions for field-independent basis sets accord with the Hellmann-Feynman theorem. In our density functional calculation the dipole moment expansion is used and the polarizability is defined by

$$\alpha_{ij} = \frac{\partial \mu_i(F)}{\partial F_j} = -\frac{\partial^2 E(F)}{\partial F_i \partial F_j} \qquad i,j = (x,y,z)$$

Using the finite difference expressions for the first and second derivatives, the diagonal elements of the polarizability tensor α_{ii} can be find from the dipole moment $\mu_{i(F)}$, or from the total energy $E(F)$ at F=0, and $\boldsymbol{F} = \pm\delta F_i$ applied along the ith axis. In the present work, the external field is applied along x, y, z axes with a magnitude of 0.005 a.u and a tighter self-consistent field (SCF) convergence of 10^{-8} hartree is adopted as a criterion. These values have been found to yield well-converged results for the polarizability. The measured data in experiments are usually the mean polarizabilities ($<\alpha>$), and it is sufficient to

compute only the diagonal components α_{ii} of the polarizability tensor, which can be obtained by the trace of the polarizability tensor to be

$$<\alpha>=\frac{1}{3}tr(\alpha_{ij})=\frac{1}{3}(\alpha_{xx}+\alpha_{yy}+\alpha_{zz})$$

Because of rotational invariance of the trace of the polarizability tensor, this value does not depend on the choice of the coordinate system. The finite field approach[20] implemented within the GAUSSIAN 03 package is used to calculate dipole moment and static electric polarizability components at B3LYP/LANL2DZ level. In the DFT framework, B3LYP functionals combined with LANL2DZ basis sets can give a good description of the bonding as well as the geometrical and electronic features of TM clusters. Thus, our method is expected to describe the tantalum clusters polarizabilities well at a level of acceptable computational precision and time.

2 Geometrical Isomers and Energy Difference

Natural Ta_2 and Ta_3 clusters have been discussed above in the Computational Details of ESI. For tantalum tetramer (Ta_4), there are three relative stable planar and three-dimensional (3D) structures gotten in our optimization. The total energies for the two 3D structures are all lower than the planar configurations'. The tetrahedron with T_d symmetry (4-a) is found to be the most stable structure from frequency analysis and corresponds to the lowest energy among the stable isomers of Ta_4 clusters. The obtained ground state of tantalum tetramer is a spin single state ($^1A_1$). However, with the same structure which is a distorted tetrahedron with C_2 symmetry, the spin triplet state isomer (^3A) is 0.520 eV above in energy than the spin single ground state. Though the "butterflylike" geometry with C_{2v} symmetry (4-b) is the next stable structure of Ta_4 cluster, it is significantly higher in energy at 1.513 eV above the ground state. The obtained planar rhombus isomer (4-c) with D_{2h} symmetry is also significantly higher in energy at 1.699 eV above the ground state. The calculated two metastable isomers (4-b and 4-c) of Ta_4 clusters are all found to be triplet state. Their single state are all unstable and did not find relative stable geometries in our calculation.

For Ta_5, the initial geometries used in our optimization are triangular bipyramid, square pyramid, and the planar structures in certain symmetry. The obtained triangular bipyramid (C_{2v}) with spin sextet state (^6A) is more stable than the square pyramid (C_{4v}) with spin sextet state ($^6B_2$) by 1.421 eV in total energy. In addition to the 3D structures, one stable planar (5-c) with C_{2v} symmetry which is significantly higher in total energy at 1.699 eV above the ground state is obtained. The obtained ground state and metastable state with different configurations for Ta_5 cluster are all spin sextet state.

The lowest energy structure for neutral Ta_6 cluster is a distorted octahedron isomer (6-a) with D_{4h} symmetry and spin triplet state ($^3A_{1g}$). The face-capped trigonal bipyramid (6-b) a slightly distorted C_{2v} octahedral configuration is the next stable structure of Ta_6, which is only 0.028 eV higher in total energy than the ground state. Thus, there exists rivalrousness for the ground state between these two isomers. In addition, this ground state with distorted octahedral isomer is a spin triplet configuration (^3A) and only 0.006 eV lower than the spin single state (^1A) in total energy with the same structure. The results demonstrate that there exists a different distorted octahedral structure and spin multiplicities with nearly degenerate energies for Ta_6 cluster. The triangular prism isomer (6-c) with D_{3h} symmetry and spin single state ($^1A_1'$) is found to be 2.022 eV less stable in total energy than the ground state. The pentagonal pyramid isomer (6-d) with C_{5v} symmetry is the next stable structure of Ta_6, which is 4.647 eV higher in energy than the lowest energy structure. Our calculation obtained three planar structures for Ta_6 cluster which are all evolved by adding one atom at different position to "W"-shaped planar of Ta_5 cluster. However, for the lowest energy planar isomer (6-e), there is still significantly higher in total energy at 4.883 eV above the 3D-structured ground state.

In the case of neutral Ta_7 cluster, the pentagonal bipyramid (PBP) geometry with D_{5h} symmetry (7-a) corresponds to the lowest-energy configuration. The face-capped octahedron structure with C_{3v} symmetry (7-b) comes next in energy which is 1.568 eV higher than the lowest-energy structure. The stable C_2 structure shown in Fig. 1 (7-c), having the highest energy for Ta_7 clusters, can be regarded as two triangular bipyramid (TBP) fused together at one trigonal face. For Ta_8, the lowest-energy structure (8-a)

is found to be a bicapped distorted octahedron with C_{2v} symmetry and spin single state (^{1}A). A distorted one-capped PBP geometry (8-b) based on the ground state of Ta_7 is only 0.966 eV higher in energy than its lowest-energy structure, and it's a spin triplet configuration (^{3}A"). A face-capped octahedron structure with C_{2v} symmetry (8-b) comes from one atom added on Ta_7 (7-b) structure, however, it's higher in energy (2.107 eV) than the lowest-energy structure of Ta_8 cluster. For Ta_8, we also obtained the most-highest energy (2.701 eV) structure (8-d) which is a three triangular bipyramid (TBP) geometry with D_{2d} symmetry evolved from Ta_7 (7-c) geometry.

For Ta_9, a tricapped prism structure with C_{3h} symmetry (9-a) is the ground state geometry. We also obtained two two-atom-capped geometry on different positions of pentagonal bipyramid (PBP), which are all higher in energy (0.115 eV for 9-b, 1.084 eV for 9-c, respectively) than the lowest-energy structure of Ta_9. For Ta_{10}, the bicapped antiprism structure with C_{2v} symmetry (10-a) and spin triplet state (^{3}A) is found to be most stable. A three-atom-capped geometry on pentagonal bipyramid (PBP) only has 0.762 eV higher in energy than its lowest-energy structure. We also calculated a capped pyramid isomer which are much higher (5.951 eV) in energy than the ground state structure. For neutral Ta_{11} cluster, the four-capped distorted pentagonal bipyramid (PBP) structure with C_{2v} symmetry (11-a) only lies 0.478 eV lower in total energy than the three-capped hexagonal bipyramid (HBP) structure with C_s symmetry (11-b). We also calculated a penta-capped prism (11-c) with C_{2v} symmetry, which only lies 0.826 eV higher in total energy than the lowest-energy structure.

For Ta_{12}, a slightly distorted empty cage icosahedron (12-a) with S_{10} symmetry and spin triplet state is found to be the lowest-lying state. The closed-lying energy structure (12-b) with C_s symmetry and spin single state (^{1}A) is regarded as capping of Ta_{11}(11-b) isomer by an apex atom. The second close-lying isomer (12-c) with C_s symmetry and spin single state (^{1}A) of Ta_{12} is regarded as capping one atom on Ta_{11} (11-a) ground state structure or a four-capped hexagonal bipyramid structure, which only lies 0.219 eV higher in energy than the isomer of Ta_{12} (12-b). The 12-d isomer is a five-capped hexagonal bipyramid structure but missing one apex atom with C_s symmetry and spin single state (^{1}A'). The 12-e isomer is a

distorted two-layer octahedron with C_{2v} symmetry, which is based on two fused triangular prisms with capping of four atoms (a different view is a distorted capped cube) with C_{2v} symmetry and spin triplet state ($^3A_2$).

The ground state of Ta_{13} cluster is a spin double state (^2A) and with C_s symmetry, which is a distorted five-capped hexagonal bipyramid (HBP) structural pattern (13-a) based on the ground states of Ta_{11}. The icosahedral isomers with distorted obviously C_1 symmetry (13-b) and distorted slightly C_{2h} symmetry (13-c), are the two following close-lying structures which are higher in total energy at 0.335 and 0.929 eV above the ground state structure (13-a), respectively. This result agrees with the previous reports for Ta_{13}.[21-23] One atom capped empty cage distorted icosahedron with C_3 symmetry (13-d) and spin quadruple state (^4A) is significantly higher in total energy at 1.903 eV above the ground state. The penta-capped prism structure (13-e) with C_{2v} symmetry and spin double state ($^2B_1$) which can be regard as evolving from adding one atom on the isomer of 11-c lies 2.301 eV higher in energy than the ground state. However, this geometry is developed to the body-centered-cubic (BCC) structure which is energetically preferred in our structure optimizations for the neutral Ta_{15} cluster.

Three degenerated isomers that competed the global minimum of Ta_{14} are found. Two of them can be derived from a 15-atom icositetrahedron with hexagonal layered structure: one misses a hexagonal surface atom and the other removes an apex atom. The former with an approximate C_s symmetry (14-a) is only 0.349 eV lower in energy than other isomer with C_{6v} symmetry (14-b). A BCC-type structure with C_{4v} symmetry (14-c) can be considered as another degenerate isomer, which lies only 0.628 eV higher in total energy than the lowest energy isomer (14-a). A hexagonal layer with center atom capped with a rhombus above and below (15-a), which is a slight distortion cubic structure is the ground state geometry for Ta15 cluster. The next isomer (15-b) with C_{2v} symmetry, which is obtained through fusing four octahedrons together, lies only 0.044 eV higher in total energy. The energy difference of these two isomers is so tiny that they can be concomitant in experiments. In addition, the two capped icosahedron isomer (15-c) of Ta_{15} are 1.448 eV higher in energy than the lowest energy structure.

Based on the capping of hexagonal bipyramid structure of Ta_{15} (15-b) with a dimer and a trimer on one of hexagonal faces, developed the lowest-energy structure for Ta_{16} (16-a) and Ta_{17} (17-a) cluster. By adding two atom on the face (16-b) and bottom (16-c) of pentagonal bipyramid structure, respectively, the two closed energy isomers of Ta_{16} cluster are slight higher in energy than its lowest-energy structure. One atom-capped cubic structure (16-d) based on Ta_{15} clusters (15-a) is only 0.876 eV higher in energy than the lowest-energy structure. Thus, we can obviously concluded that the obtained three isomers are the competitive candidates of the ground state for Ta_{16} clusters. A capped decahedron (17-b) is the first close-lying isomer of Ta_{17}, lying 1.567 eV higher in energy. And the two atom-capped on cubic structure (17-c) formed from 15-a and 16-d is much higher in energy (2.559 eV) than the lowest-energy structure.

Table S1 The calculated parameters for all obtained stable isomers of neutral Ta_n(n=2-17) clusters, and their geometries, symmetry, spin multiplicities (S), the total energy (E), binding energy per atom (E_b/n), the energy gap of HOMO-LUMO (E_{gap}), electric dipole moment (EDM), mean static dipole polarizabilities per atom ($\langle\alpha\rangle/n$), vibrational frequencies for the most clear six vibrational peaks, and zero-point vibrational energies (ZPVEs).

n	Isomer	Geometry (Symmetry)	S	E (a.u.)	E_b/n (eV)	E_{gap} (eV)	EDM (Debye)	$\langle\alpha\rangle/n$ (Å^3)	Vibrational frequencies (cm^{-1})	ZPVEs (eV)
2		Dimer($D_{\infty h}$)	5	-115.382	1.448	2.450	0.000	68.181	285.42	0.018
3		Equilateral triangle(D_{3h})	6	-173.180	2.412	2.318	0.000	66.190	174.95, 174.98, 257.23	0.038
		Linear chain ($C_{\infty v}$)	6	-173.081	1.520	1.764	0.005	73.779	34.74, 136.46, 168.81	0.021
4	4-a	Distorted tetrahedron(C_2)	1	-231.030	3.253	1.504	0.579	56.961	106.05, 106.13, 180.64, 183.39, 192.67	0.065
	4-b	"Butterflylike"(C_{2v})	3	-230.974	2.875	1.759	0.400	59.060	64.91, 145.28, 155.01, 226.52, 248.76	0.060
	4-c	Planar rhombus(D_{2h})	3	-230.967	2.829	1.323	0.019	67.345	120.68, 127.23, 168.42, 238.86, 247.93	0.056
5	5-a	Triangular bipyramid (C_{2v})	6	-288.803	3.342	1.710	0.000	65.391	81.14, 138.49, 143.16, 143.16, 212.48	0.083
	5-b	Square pyramid (C_{2v})	6	-288.751	3.058	1.041	0.168	89.115	54.20, 58.58, 154.11, 154.13, 245.37	0.063
	5-c	"W"-shaped planar(C_{2v})	6	-288.717	2.873	1.300	0.841	63.941	18.51, 110.73, 111.85, 120.56, 142.05	0.074
6	6-a	Distorted octahedron(D_{4h})	3	-346.653	3.748	1.525	0.000	57.041	32.92, 189.04, 196.92	0.104
	6-b	Face-capped TBP(C_{2v})	3	-346.652	3.743	1.340	0.085	58.936	55.30, 88.54, 186.51, 189.83, 221.41	0.108
	6-c	Triangular prism(D_{3h})	1	-346.579	3.411	1.879	0.000	54.569	130.31, 183.35, 183.35, 261.75	0.101
	6-d	Pentagonal pyramid(C_{5v})	1	-346.483	2.973	0.370	0.806	63.954	137.50, 146.30, 146.56, 214.55, 214.84, 220.74	0.092
	6-e	Distorted rhombus(C_{2h})	1	-346.474	2.934	0.830	0.000	70.217	8.989, 66.16, 108.27, 162.52, 249.67	0.090
7	7-a	PBP(D_{5h})	4	-404.500	4.023	0.880	0.001	50.606	94.50, 169.96, 173.42, 173.46, 208.94	0.103
	7-b	Face-capped octahedron(C_{3v})	4	-404.442	3.800	1.416	1.155	55.369	79.43, 79.48, 118.99, 128.44, 138.28, 204.30	0.126
	7-c	Two TBP(C_2)	4	-404.426	3.734	1.278	0.268	59.806	70.72, 95.24, 96.36, 128.45, 143.23, 174.56	0.123
8	8-a	Bi-capped octahedron(C_{2v})	1	-462.311	4.110	1.400	0.876	51.379	105.09, 109.57, 135.52, 177.58, 188.03, 211.30	0.171
	8-b	Singly capped PBP(C_s)	3	-462.276	3.989	1.367	0.476	55.167	83.22, 97.37, 118.37, 137.91, 146.65, 196.84	0.156
	8-c	Bi-capped octahedron(C_{2v})	1	-462.234	3.847	1.091	2.627	57.423	99.77, 118.15, 123.34, 125.91, 153.43, 157.40	0.161
	8-d	Tetra-capped tetrahedron(D_{2d})	1	-462.212	3.773	1.048	0.000	54.056	107.73, 131.19, 140.77, 190.22, 200.55	0.139
9	9-a	Tri-capped prism(C_{3h})	4	-520.112	4.147	1.549	0.002	51.075	133.01, 133.17, 177.32, 177.40, 178.12, 203.56	0.189
	9-b	Bi-capped PBP(C_{2v})	4	-520.108	4.134	1.093	1.686	55.522	64.34, 94.36, 119.51, 127.63, 167.63, 171.26	0.178
	9-c	Bi-capped PBP(C_{2v})	4	-520.069	4.016	1.217	1.431	54.617	43.84, 136.70, 175.96, 179.62, 213.42, 223.49	0.171
10	10-a	Bi-capped antiprism(C_{2v})	3	-577.952	4.282	1.653	0.554	49.517	101.18, 160.89, 167.10, 172.29, 180.03, 209.65	0.215
	10-b	Tri-capped PBP(C_{3v})	5	-577.924	4.206	1.300	2.872	60.217	108.37, 108.61, 133.32, 133.45, 217.78, 217.93	0.187

	10-c	Tetra-capped octahedron(T_d)	1	-577.733	3.687	1.049	0.000	59.993	58.48, 109.32, 172.79, 238.83,	0.195
11	11-a	Tetra-capped PBP(C_{2v})	4	-635.751	4.292	1.556	1.727	53.410	40.27, 77.87, 100.79, 123.63, 141.07, 154.81	0.223
	11-b	Tri-capped HBP(C_s)	4	-635.734	4.249	0.709	0.864	54.574	82.08, 91.32, 129.41,160.24, 164.13, 211.88	0.238
	11-c	Penta-capped prism(C_{2v})	2	-635.721	4.217	1.108	2.528	58.020	85.59, 119.60, 170.13, 173.22, 184.73, 217.78	0.239
12	12-a	Distorted icosahedron(S_{10})	1	-693.604	4.420	1.893	0.254	52.237	50.66, 79.92, 91.61, 121.07, 151.81, 167.99	0.260
	12-b	Five-capped PBP(C_s)	1	-693.571	4.346	1.105	1.154	53.819	32.25, 53.60, 118.29, 172.17, 187.94, 210.09	0.252
	12-c	Four-capped HBP(C_s)	1	-693.563	4.328	0.933	2.344	52.710	75.88, 95.64, 109.64, 117.82, 154.97, 165.65	0.252
	12-d	Five-capped HBP missing an apex atom (C_s)	1	-693.488	4.159	0.963	0.584	56.405	53.24, 127.70, 167.57, 170.97, 193.71, 210.77	0.244
	12-e	Distorted capped cube (C_{2v})	3	-693.471	4.120	0.921	1.057	54.183	114.45, 136.45, 142.73, 163.14, 193.15, 233.01	0.229
13	13-a	Five-capped HBP(C_s)	2	-751.408	4.429	1.224	0.608	53.448	66.48, 81.53, 114.27, 162.19, 165.86, 192.84	0.287
	13-b	Distorted icosahedron (C_1)	2	-751.396	4.404	1.216	1.877	54.105	164.16, 170.73, 202.74, 217.55, 228.13, 250.85	0.268
	13-c	Distorted icosahedron (C_{2h})	2	-751.374	4.358	1.065	0.000	56.565	153.90, 156.12, 164.71, 231.00, 277.69, 282.94	0.249
	13-d	Singly capped empty cage icosahedron(C_s)	4	-751.368	4.345	1.150	3.212	52.394	81.24, 101.43, 117.07, 144.65, 163.35, 182.99	0.281
	13-e	BCC(C_{2v})	2	-751.324	4.252	0.805	0.431	60.997	57.13, 84.42, 110.05, 140.65, 173.36, 182.99	0.253
14	14-a	Icositetrahedron missing an apex atom(C_s)	1	-809.244	4.498	0.947	1.839	52.232	97.38, 115.13, 119.37, 138.37, 160.81, 242.0	0.281
	14-b	Icositetrahedron missing a hexagonal surface atom(C_{6v})	3	-809.231	4.473	0.902	0.734	55.060	89.16, 89.49, 98.12, 124.30, 125.77, 126.32	0.275
	14-c	BCC(C_{4v})	1	-809.219	4.449	0.922	0.701	52.016	90.99, 91.06, 147.12, 159.99, 160.04, 174.01	0.316
15	15-a	Distorted quartet BCC(C_s)	2	-867.072	4.543	1.189	0.554	52.323	138.36, 142.82, 164.97, 165.37, 220.81, 230.92	0.332
	15-b	Icositetrahedron(C_3)	4	-867.071	4.541	0.801	1.478	60.068	60.61, 105.46, 127.00, 130.85, 159.21, 230.96	0.293
	15-c	Bi-capped icosahedron(C_2)	4	-867.020	4.447	1.061	1.636	56.524	26.28, 83.14, 98.50, 126.74, 159.01, 240.41	0.309
16	16-a	Capped icositetrahedron(C_s)	1	-924.866	4.524	0.963	2.248	54.648	60.26, 152.65, 169.23, 174.67, 222.13, 243.55	0.326
	16-b	Bi-capped icositetrahedron missing an apex atom(C_s)	1	-924.856	4.508	0.958	1.160	53.389	98.34, 104.07, 121.91, 158.37, 180.61, 194.19	0.348
	16-c	Tri-capped icosahedron(C_1)	3	-924.843	4.485	0.928	1.730	54.301	40.99, 54.19, 58.96, 108.81, 180.32, 203.28	0.307
	16-d	Capped BCC(C_1)	1	-924.834	4.470	0.784	3.078	52.254	53.32, 102.50, 121.87, 132.92, 232.28, 243.22	0.331
17	17-a	Bi-capped icositetrahedron (C_s)	2	-982.718	4.602	0.820	3.116	52.459	38.60, 114.30, 122.54, 165.78, 192.80, 221.45	0.353
	17-b	Four-capped icosahedron(C_1)	2	-982.661	4.509	0.851	0.976	54.342	38.66, 45.74, 97.78, 147.99, 157.01, 229.64	0.354

17-c	Bi-capped BCC(C_1)	2	-982.624	4.451	1.019	2.119	52.652	71.36, 116.07, 180.15, 197.11, 211.80, 222.80	0.341

Figure S1 The *s*-, *p*-, *d*-projected partial density of states and total density of states for the lowest energy structure of representative Ta_n clusters with n=7, 10, 13 and 15 along with the corresponding HOMO and LUMO orbitals surfaces. (The dashed orange lines refer to the Fermi levels.)

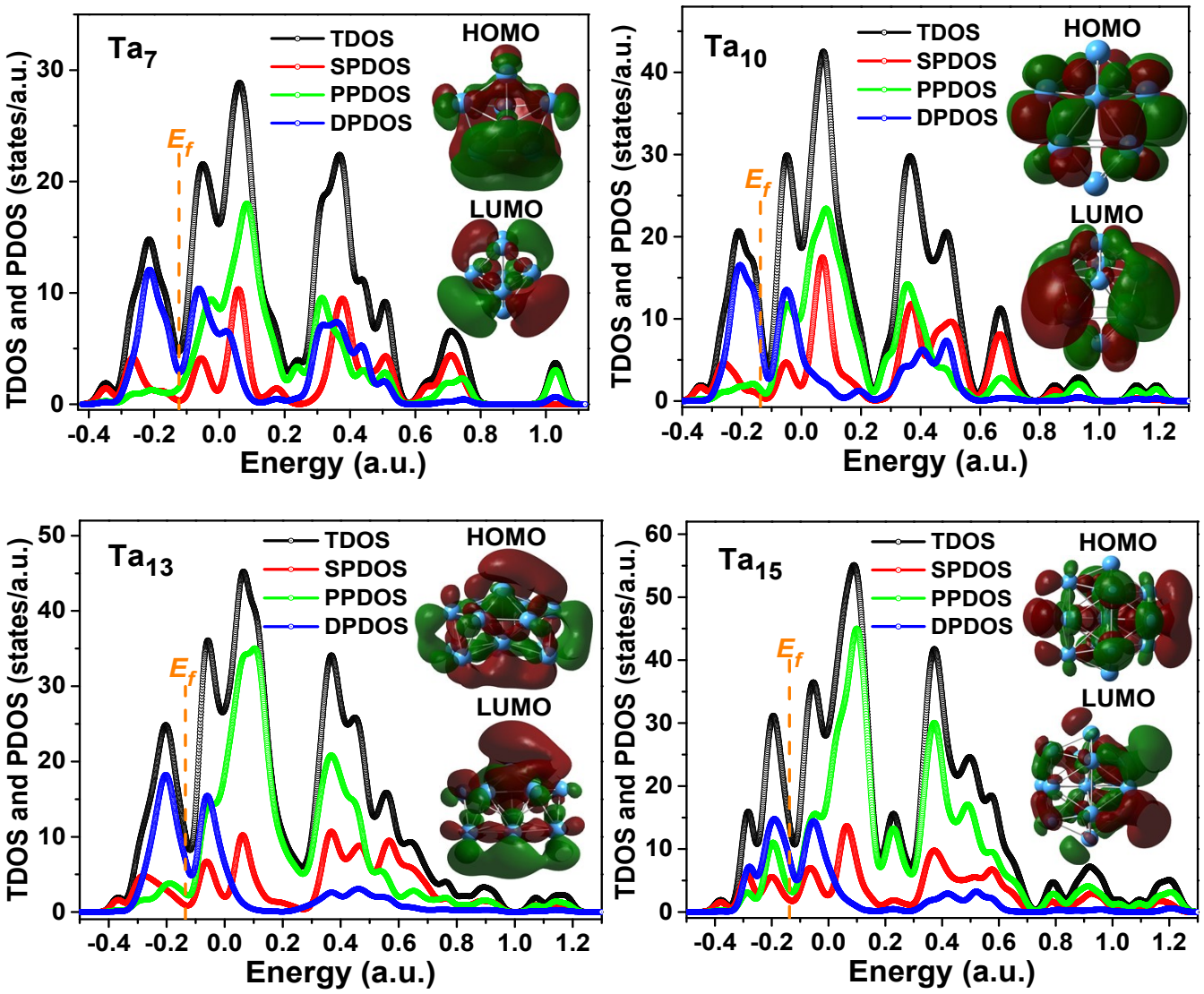

References

1 Xiyuan Sun, Jiguang Du, Pengcheng Zhang and Gang Jiang, A Systemic DFT Study on Several 5d-Electron Element Dimers: Hf_2, Ta_2, Re_2, W_2, and Hg_2, *J. Clust. Sci.*, 2010, **21**, 619−636.

2 P. Jeffrey Hay and Willard R. Wadt, Ab initio effective core potentials for molecular calculations. Potentials for K to Au including the outermost core orbitals, *J. Chem. Phys.*, 1985, **82**, 299−310.

3 Xi-Bo Li, Hong-Yan Wang, Xiang-Dong Yang, Zheng-He Zhu and Yong-Jian Tang, Size dependence of the structures and energetic and electronic properties of gold clusters, *J. Chem. Phys.*, 2007, **126**, 084505.

4 Xi-Bo Li, Hong-Yan Wang, Ran Lv, Wei-Dong Wu, Jiang-Shan Luo and Yong-Jian Tang, Correlations of the Stability, Static Dipole Polarizabilities, and Electronic Properties of Yttrium Clusters, *J. Phys. Chem. A*, 2009, **113**, 10335−10342.

5 Bin Wang, Hua-Jin Zhai, Xin Huang and Lai-Sheng Wang, On the Electronic Structure and Chemical Bonding in the Tantalum Trimer Cluster, *J. Phys. Chem. A*, 2008, **112**, 10962−10967.

6 Michael W. Heaven, Gerarda M. Stewart, Mark A. Buntine and Gregory F. Metha, Neutral Tantalum-Carbide Clusters: A Multiphoton Ionization and Density Functional Theory Study, *J. Phys. Chem. A*, 2000, **104**, 3308−3316.

7 Z. J. Wu, Y. Kawazoe and J. Meng, Geometries and electronic properties of Ta_n, Ta_nO and TaO_n (n=1–3) clusters, *J. Mol. Struct.: THEOCHEM*, 2006, **764**, 123−132.

8 Christopher J. Barden, Jonathan C. Rienstra-Kiracofe and Henry F. Schaefer III, Homonuclear 3d transition-metal diatomics: A systematic density functional theory study, *J. Chem. Phys.*, 2000, **131**, 690−700.

9 Z. J. Wu, Density functional study of the second row transition metal dimers, *Chem. Phys. Lett.*, 2004, **383**, 251−255.

10 Michael D. Morse, Clusters of Transition-Metal Atoms, *Chem. Rev.*, 1986, **86**, 1049−1109.

11 B. A. Collings, D. M. Rayner and P. A. Hackett, Ionization potentials of tantalum clusters with three to 64 atoms, *Int. J. Mass Spectrom. Ion Processes*, 1993, **125**, 207−214.

12 Zhendong Hu, Bo Shen, J. R. Lombardi and D. M. Lindsay, Spectroscopy of mass-selected tantalum dimers in argon matrices, *J. Chem. Phys.*, 1992, **96**, 8757−8760.

13 Joseph L. Jules and John R. Lombardi, Transition Metal Dimer Internuclear Distances from Measured Force Constants, *J. Phys. Chem. A*, 2003, **107**, 1268−1273.

14 Wei Fa, Chuanfu Luo, and Jinming Dong J, Coexistence of ferroelectricity and ferromagnetism in tantalum clusters, *J. Chem. Phys.*, 2006, **125**, 114305.

15 Li Fang, Xiaole Shen, Xiaoyu Chen and John R. Lombardi, Raman spectra of ruthenium and tantalum trimers in argon matrices, *Chem. Phys. Lett.*, 2000, **332**, 299−302.

16 Viktoras Dryza, M. A. Addicoat, Jason R. Gascooke, Mark A. Buntine and Gregory F. Metha, Ionization Potentials of Tantalum-Carbide Clusters: An Experimental and Density Functional Theory Study, *J. Phys. Chem. A*, 2005, **109**, 11180−11190.

17 Karl Jug, Bernd Zimmermann, Patrizia Calaminici and Andreas M. Köster, Structure and stability of small copper clusters, J. Chem. Phys. 2002, **116**, 4497−4507.

18 R. G. Parr and W. Yang, *Density Functional Theory of Atoms and Molecules*, Oxford University Press, New York, 1989.

19 Robert G. Parr, Robert A. Donnelly, Mel Levy and William E. Palke, Electronegativity: The density functional viewpoint, *J. Chem. Phys.*, 1978, **68**, 3801-3807.

20 Henry A. Kurtz, James J. P. Stewart and Kenneth M. Dieter, Calculation of the Nonlinear Optical Properties of Molecules, *J. Comput. Chem.*, 1990, **11**, 82-87.

21 Henrik Grönbeck, Arne Rosén and Wanda Andreoni, Structural, electronic, and vibrational properties of neutral and charged Nb_n (n=8, 9, 10) clusters, *Phys. Rev. A*, 1998, **58**, 4630.

22 Yan Sun, Min Zhang and René Fournier, Periodic trends in the geometric structures of 13-atom metal clusters, *Phys. Rev. B*, 2008, **77**, 075435.

23 Min Zhang and René Fournier, Density-functional-theory study of 13-atom metal clusters M_{13}, M=Ta–Pt, *Phys. Rev. A*, 2009, **79**, 043203.